Thermal valence-bond-solid transition of quantum spins in two dimensions

Songbo Jin and Anders W. Sandvik

Phys. Rev. B **87**, 180404 — Published 22 May 2013

DOI: 10.1103/PhysRevB.87.180404

Thermal valence-bond-solid transition of quantum spins in two dimensions

Songbo Jin and Anders W. Sandvik
Department of Physics, Boston University, 590 Commonwealth Avenue, Boston, Massachusetts 02215, USA
(Dated: May 6, 2013)

We study the $S = 1/2$ Heisenberg (J) model on the two-dimensional (2D) square lattice in the presence of additional higher-order spin interactions (Q) which lead to a valence-bond-solid (VBS) ground state. Using quantum Monte Carlo simulations, we analyze the thermal VBS transition. We find continuously varying exponents, with the correlation-length exponent ν close to the Ising value for large Q/J and diverging when Q/J approaches the quantum-critical point (the critical temperature $T_c \to 0$). We identify the transition with a class of conformal field theories with charge $c = 1$ and critical exponents varying between those of the 2D Ising model and the Kosterlitz-Thouless (KT) fixed point. We find explicit evidence for KT physics by studying the emergence of $U(1)$ symmetry of the order parameter at $T = T_c$ when $T_c \to 0$.

PACS numbers: 75.10.Kt, 75.10.Jm, 75.40.Mg, 75.40.Cx

The $S = 1/2$ Heisenberg model on the two-dimensional (2D) square lattice can host a quantum phase transition between a Néel antiferromagnet (AFM) and a valence-bond-solid (VBS) when other interactions are added[1]. This transition between two different ordered ground states has been the subject of a large body of work[2]. In the J-Q model[3], the pair exchange J is supplemented by products of two or more singlet projectors on adjacent links, with strength Q. For large Q/J the correlated singlets destroy the AFM order, leading to the VBS crystallization of singlets. Unlike geometrically frustrated systems, on which research on VBS states, and the AFM–VBS transition were focused for a long time[4–7], the J-Q model is amenable to large-scale quantum Monte Carlo (QMC) simulations[8] and its AFM–VBS transition has been studied extensively[3,9–18]. The model may realize the unusual ("non-Landau") deconfined quantum-critical (DQC) point proposed by Senthil et al.[19,20], where both order parameters arise out of emergent spin-1/2 objects (spinons), which at criticality are described by a CP^1 gauge-field theory. Other, less exotic scenarios have also been put forward, however[11,21,22].

The putative DQC point is a manifestation of quantum effects, due to Berry phases and emergent topological conservation laws[20,23] that potentially are at play in many strongly-correlated quantum systems. Amenable to unbiased QMC simulations, J-Q models offer unique opportunities to examine the DQC proposal in detail from various angles. Here we present results for the VBS transition at finite temperature ($T > 0$), discussing its universality, relationship to conformal field theory (CFT), and the emergent U(1) symmetry[20] associated with the DQC point when approached at $T > 0$.

Universality of the VBS transition—The square-lattice columnar VBS obtaining with the standard J-Q model breaks Z_4 symmetry and, thus, it should exist $T > 0$. Thermal 2D Z_4-breaking transitions normally do not have fixed critical exponents, but belong to a universality class of CFTs with charge $c = 1$ exhibiting continuously varying exponents[24,25]. Realizations of these transitions include the standard XY model with a field $h\cos(4\theta_i)$ (with spin angles θ_i)[26,27], the Ashkin-Teller model[28,29], and the Ising model with nearest- and next-nearest neighbor interactions (the J_1-J_2 model)[30,31]. The deformed XY model has a critical line connecting Ising and Kosterlitz-Thouless (KT) fixed points[32,33], while the critical lines of the AT and J_1-J_2 models connect Ising and 4-state Potts points. It is intersting to ask if any of these scenarios are realized by the $T > 0$ VBS transitions of the J-Q model. In this Letter we present strong evidence for an Ising–KT critical line, with the KT transition obtaining when Q/J approaches its quantum-critical value and the critical temperature $T_c \to 0$. This agrees with the DQC U(1) gauge-field description, where the nature of the VBS state is dictated by a dangerously irrelevant operator[2,19,20], which implies that the VBS fluctuations should cross over from Z_4 to U(1) symmetric as the DQC point is approached. This has been observed in ground-state studies of the VBS fluctuations of J-Q models[3,11,12]. We here study the emergent U(1) along the critcal line when $T_c \to 0$.

The $T > 0$ VBS transition was previously studied by Tsukamoto *et al.*[34] by QMC simulations of the J-Q_2 model, where the Q_2 interaction is a product of two singlet projectors. The results showed puzzling deviations from the "weak universality" applying to the transitions discussed above, where the critical correlation-function exponent $\eta = 1/4$ but other exponents depend on system details. Instead, $\eta \approx 0.5$ was obtained[34]. Here we consider the J-Q_3 model[12], where the Q_3 terms consist of stacked bond-singlet projectors on three adjacent lattice links. This model has a more robust $T = 0$ VBS for large Q_3, while the J-Q_2 model is near-critical even for $Q_2/J \to \infty$. With the J-Q_3 model we can systematically study the $T > 0$ transition both far from the DQC point and close to it. We find $\eta = 1/4$ to high precision.

Model and methods—We next discuss the QMC calculations and data analysis on which we base our conclusions. The J-Q_3 Hamiltonian is defined as

$$H = -J \sum_{\langle i,j \rangle} P_{ij} - Q_3 \sum_{\langle ijklmn \rangle} P_{ij} P_{kl} P_{mn}, \qquad (1)$$

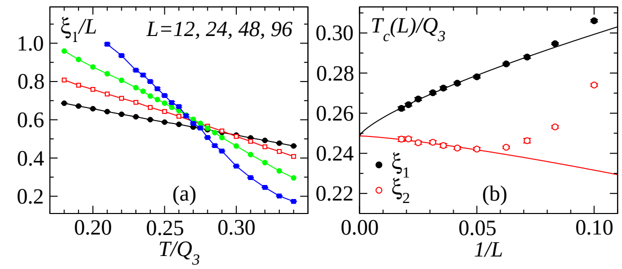

FIG. 1. (Color online) Extraction of T_c for system at $q = 5$. Shown in (a) are, in order of higher to lower curves on the left side, results for ξ_1/L versus T for system sizes $L = 96, 48, 24$, and 12. Crossing points giving $T_c(L)$ estimates are shown in (b), using both ξ_1 and ξ_2 with sizee pairs $(L, 2L)$. The data were fit to the form $T_c(L) = T_c(\infty) + a/L^w$ in the range $1/L \in [0, 0.08]$ (ξ_1) and $[0, 0.06]$ (ξ_2), yelding $T_c = 0.249(3)$ in the case of χ_1. For the ξ_2 fit, $T_c(\infty) = 0.249$ was fixed.

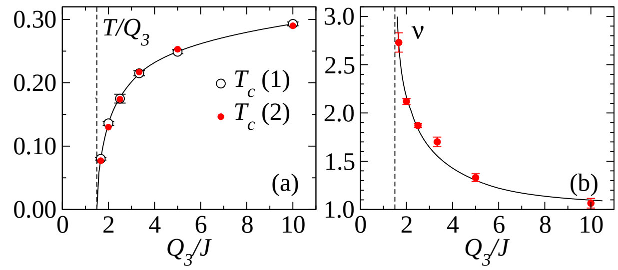

FIG. 2. (Color online) (a) The critical temperature extracted from ξ_1/T (open circles). Also shown are results (solid circles) where the VBS susceptibility exhibits the best scaling behavior when $\gamma = 7/4$ is fixed. (b) The exponent ν versus q. The vertical dashed lines in both panels mark the quantum-critical ratio q_c[12]. The curves are guides to the eye.

where P_{ij} is a nearest-neighbor bond-singlet projector;

$$P_{ij} = \tfrac{1}{4} - \mathbf{S}_i \cdot \mathbf{S}_j, \tag{2}$$

here on the square lattice with L^2 sites. We define the coupling ratio $q = Q_3/J$. The point separating the AFM and VBS ground states is $q_c = 1.500(2)$[12]. We use the stochastic series expansion (SSE) QMC method with loop updates[35–37] to compute quantities useful for extracting the critical temperature and exponents of the $T > 0$ VBS transition for $q > q_c$.

We define the VBS correlation length using the J-term (bond) susceptibility,

$$\chi_{b_1,b_2} = \int_0^\beta d\tau \langle P_{b_2}(\tau) P_{b_1}(0) - \langle P_b\rangle^2 \rangle, \tag{3}$$

where P_b is a singlet projector (2), with b a bond connecting sites i_b, j_b. The susceptibilities can be computed easily with the SSE method, because the projectors are terms of the Hamiltonian and, thus, appear in the sampled operator sequences. With $n(b)$ denoting the number of J-operators on bond b, the susceptibility is[38]

$$\chi_{b_1,b_2} = \langle n(b_1)n(b_2) - \langle n(b)\rangle^2 - \delta_{b_1,b_2} n(b_1)\rangle/\beta. \tag{4}$$

This estimator works well when q is not too large. When $q > 10$ the measurements become noisy due to the low density of J-operators.

To detect columnar VBS order, we consider the bonds b_1 and b_2 oriented in the same (x or y) lattice direction and denote by $\chi^\alpha(\mathbf{r})$, $\alpha = x, y$, the spatially averaged distance-dependent susceptibility. The VBS susceptibility $\chi^x_{\rm VBS}$ is the $\mathbf{q} = (\pi, 0)$ Fourier transform of $\chi^x(\mathbf{r})$ (and analogously for y). The columnar VBS breaks the lattice rotational symmetry, and we can define two correlation lengths. Using the x susceptibility and defining $\mathbf{q}_0 = (\pi, 0)$, $\mathbf{q}_1 = (\pi + 2\pi/L, 0)$ and $\mathbf{q}_2 = (\pi, 2\pi/L)$ we have the correlation lengths parallel and perpendicular to the x bonds for an $L \times L$ lattice;

$$\xi_1^x = \frac{L}{2\pi}\sqrt{\frac{\chi^x_{\rm VBS}(\mathbf{q}_0)}{\chi^x_{\rm VBS}(\mathbf{q}_1)} - 1}, \quad \xi_2^x = \frac{L}{2\pi}\sqrt{\frac{\chi^x_{\rm VBS}(\mathbf{q}_0)}{\chi^x_{\rm VBS}(\mathbf{q}_2)} - 1}, \tag{5}$$

and analogously for y. Average valuess of x, y quantities are denoted in the following without superscript.

Critical temperature—To illustrate how T_c is determined, Fig. 1(a) shows ξ_1/L versus T at $q = 5$ for several system sizes. According to finite-size scaling theory[39], ξ_1/L for different L should cross at T_c when $L \to \infty$. Due to scaling corrections, the crossing point $T_c(L_1, L_2)$ between two system sizes, which we here take as L and $2L$, drifts slowly with L and converges as the system size increases. We use the crossing point for both ξ_1 and ξ_2 to extract T_c and check the consistency of the two results.

Fig. 1(b) shows two sets of $T_c(L)$ point obtaied from ξ_1 and ξ_2. Both curves can be fitted with the form $T_c(L) = T_c(\infty) + a/L^w$ but the parameters are different. The two curves appoach T_c from different directions. The ξ_1 data have large deviations from the fitted function only for small systems ($L \lesssim 12$), while ξ_2 shows corrections extending up to larger L and the size dependence is non-monotonic. The data nevertheless extrapolate consistently to a common T_c in the thermodynamic limit. To demonstrate this, we show in Fig. 1(b) a fit to the ξ_1 data, giving $T_c = 0.249(3)$. (which has a smaller statistical error than the value from ξ_2). We also show a fit to the ξ_2 data, where $T_c(\infty)$ is fixed at the result from ξ_1.

Results for other q points were extracted in the same way, making sure that ξ_1 and ξ_2 data extrapolate consistently and using the ξ_1 results (which always have smaller errors) for further analysis. This procedure becomes increasingly challenging as the quantum-critical point q_c is approached and $T_c \to 0$. The corrections to the asymptotic form became more profound and larger systems have to be used. In addition, the SSE calculations become more time-consuming, since $L \gg 1/T$ is required for the simulated effective classical system to be firmly in the 2D limit. The largest system was $L = 192$ at $q = 5/3$. T_c is shown versus q in Fig. 2(a).

Critical exponents—we next present an analysis of the

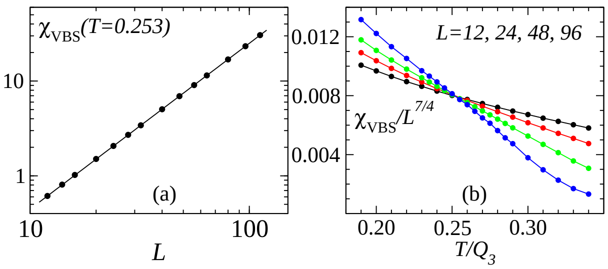

FIG. 3. (Color online) (a) Scaling behavior of the critical VBS susceptibility for systems at $q = 5$. Here T was adjusted to give the best linear scaling on the log-log plot, giving $\gamma/\nu = 1.750(1)$. (b) The size-scaled susceptibility under the assumption $\eta = 1/4$ versus T for several system sizes. The crossing point is consistent with T_c extracted from the correlation length.

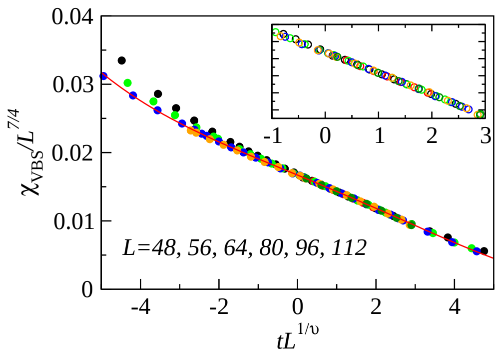

FIG. 4. (Color online) Data collapse of the VBS susceptibility for system s at $q = 10/3$. The inset shows data for $L = 80, 96, 112$ in the range $tL^{1/\nu} \in [-0.5, 3]$ for which the fitting procedure was carried out. The main part shows data in a larger window and including also smaller systems. The fit yelded $\nu = 1.70(5)$.

scaling behavior of the VBS susceptibility, which exactly at T_c should follow the form

$$\chi_{\mathrm{VBS}}(T_c) \sim L^{\gamma/\nu}, \tag{6}$$

where $\gamma/\nu = 2 - \eta$. Here we can use T_c extracted above from the correlation length scaling. Alternatively, we can adjust the temperature until the best power-law scaling is obtained. If sufficiently large system sizes are used the two methods should of course deliver consistent results. This is indeed the case, as shown in Fig. 2(a). An example of the best power-law scaling is shown for $q = 5$ in Fig. 3(a). Here the corrections to scaling appear to be very small (i.e., a straight line can be well fitted on the log-log scale even when systems as small as $L = 10$ are included) and the temperature, $T = 0.253$, is only an error bar off the T_c value extracted from ξ_1/L. A series of fits with a bootstrap analysis to estimate the errors yielded $\gamma/\nu = 1.750(1)$, or $\eta = 0.250(1)$. We find consistency with $\eta = 1/4$ at similar level of precision for all q values studied.

Fig. 3(b) demonstrates a different way to analyze the susceptibility and test the assumption $\eta = 1/4$, by graphing $\chi_{\mathrm{VBS}}L^{-7/4}$ versus T is for different system sizes. All curves cross essentially at the same point, which confirms the scaling power $\gamma/\nu = 7/4$ in Eq. (6). The remarkable absence of drift in the crossing points of $\chi_{\mathrm{VBS}}L^{-7/4}$ (in contrast to the significant drift found for the normalized correlations lengths) makes this quantity a perfect candidate for carrying out a finite-size data collapse to extract correlation length exponent ν, which we consider next.

Shown in Fig. 4 are data sets for system sizes $L = 48$ to 112 at $q = 10/3$, graphed versus $tL^{1/\nu}$, where t is the reduced temperature, $t = (T - T_c)/T_c$, and the critical temperature was determined in the manner above to be $T_c = 0.217$. The correlation lengt ν was adjusted to give the best data collapse, as measured with respect to a polynomial fitted simultaneously to all data points for $L = 80, 96, 112$ in the range $tL^{1/\nu} \in [-0.5, 3]$. A zoom-in on this window is shown in the inset. The fit was restricted to the larger sizes in order to minimize the effects of neglected scaling corrections, and the window of $tL^{1/\nu}$ values was chosen to obtain a statistically sound fit. This procedure along with an analysis of the statistical errors gave $\nu = 1.70(5)$. When q is tuned towards q_c, larger system sizes are required to achieve good collapse due to more pronounced scaling corrections, as already mentioned above. As an example, at $q = 5/3$, we used system sizes $L = 112, 128, 160, 192$.

All our results for T_c and ν versus q are shown in Fig. 2. T_c clearly decreases when q approaches q_c and ν grows rapidly, changing from 1.065(5) at $q = 10$ to 2.7(1) at $q = 5/3$. The behavior suggests that ν diverges when $q \to q_c$, which would mean that the critical line corresponds to the $c = 1$ Ising–KT scenario, with the KT universality applying in the limit $q \to q_c^+$ and 2D Ising universality ($\nu = 1$) applying in the extreme limit far from the quantum-critical point (which cannot strictly be achieved within the J-Q_3 model, but ν is already close to the Ising value for $q = 10$; the largest q studied here). This scenario is also supported by the fact that there is no specific-heat peak at T_c, i.e., the exponent $\alpha < 0$.

Emergent U(1) symmetry—The varying critical exponents are related to evolving critical VBS fluctuations. We investigate these by following the distribution of the components (D_x, D_y) of the VBS order parameter. The columnar VBS operator for x-bonds are defined as

$$\hat{D}_x = \frac{1}{N}\sum_{\mathbf{r}}(-1)^x P_{\mathbf{r},\mathbf{r}+\hat{\mathbf{x}}}, \tag{7}$$

and $\hat{D}_y$ is defined analogously. An SSE-sampled configuration can be assigned definite "measured" values (D_x, D_y) by the operator-counting procedure discussed above in the context of the susceptibility (3). We accumulate the probability distribution $P(D_x, D_y)$, which reflects the nature of the VBS fluctuations. In analogy with XY models with dangerously-irrelevant Z_4 perturbations[40], one would expect the four-fold symmetric VBS distribution to develop signatures of U(1) symmetry. This has previously been observed when approaching the quantum-critical point at $T = 0$. We now

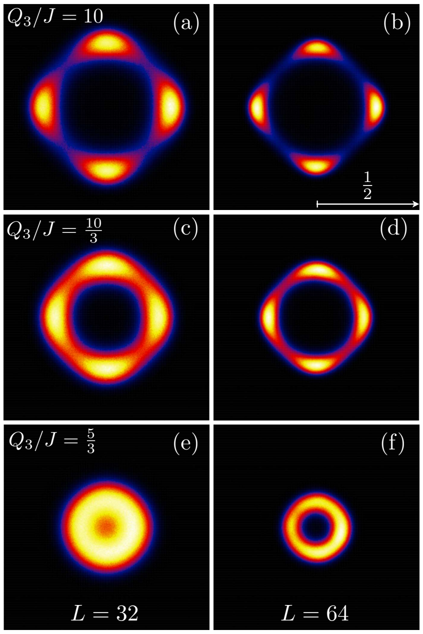

FIG. 5. (Color online) Dimer-order distribution $P(D_x, D_y)$ for system size $L = 32$ (left panels) and $L = 64$ (right panels) in the close vicinity of T_c. The coupling ratios (temperatures) are $q = 10$ ($T = 0.29$) in (a),(b); $q = 10/3$ ($T = 0.218$) (c),(d); $q = 5/3$ ($T = 0.08$) in (e),(f). In (f) the distributions is somewhat affected by unequal sampling (due to long QMC autocorrelation times) in different angular sectors.

approach this point by following the $T > 0$ critical line. Fig. 5 shows results for several combinations of the system size and the coupling ratio. While clearly four-fold symmetric distributions apply for large q, the histograms become more circular as the quantum-critical point is approached. Like at $T = 0$[12], one can expect the distribution to be effectively U(1) symmetric when L (or some other the course-graining scale) is less than a lengt-scale Λ, with $\Lambda \to \infty$ as $q \to q_c$. For the system sizes studied, $L < \Lambda$ at $q = 5/3$, while for the larger q in Fig. 5 the system sizes exceed Λ. These observations provides direct evidence for U(1)-symmetric VBS fluctuations leading to the large ν found here close to q_c.

Discussion—All our calculations show consistently that the thermal VBS transition in the J-Q_3 model has critical exponents varying in a range expected in a particular subclass of $c = 1$ CFTs. The exponent η is constant at $\eta = 1/4$, in agreement with weak universality, and ν grows rapidly as the quantum-critical point is approached, indicating an emergent U(1) symmetry of the VBS order parameter and a KT transition obtaining in the limit $T_c \to 0^+$. We expect that the same behavior should apply also in the J-Q_2 model, but that cross-over behaviors associated with the proximity to the quantum-critical point for all Q_2/J in that model may make it difficult to extract the exponents there[34]. Since microscopic details should not matter, by universality our results should apply to a wide range of VBSs.

The significance of establishing the nature of the $T > 0$ critical line is that it puts the phase diagram of the J-Q model firmly within an established CFT. For $T \to 0^+$, the effective $(2+1)$D system, obtained in a quantum–classical mapping through the path integral, is still finite in the "time" dimensions, and, thus, the KT scenario can apply. Exactly at $T = 0$ the effective system is fully 3D and a different criticality must apply (that of the putative DQC point). While we cannot strictly rule out a change of behavior to a first-order transition for very low temperatures[11,14,22] (i.e., the $c = 1$ CFT mapping would hold only down to some low temperature), there are no indications of this in any of our results. Note, in particular, that in finite-size scaling at a first-order transition one should see $\nu = 1/d$[41], where d is the dimensionality (i.e., $d = 2$ in our case when $T_c > 0$). Instead, at the lowest T_c reached here, $\nu \approx 3$.

The non-commutability of the limits $L \to \infty$ and $1/T \to \infty$ is also associated with interesting cross-overs, which we have observed here but not studied in detail. Further investigations of this aspect of the AFM–VBS transition are warranted.

Acknowledgments—This research was supported by the NSF under Grant No. DMR-1104708.

[1] N. Read and S. Sachdev, Phys. Rev. Lett. **62**,1694 (1989).
[2] For a review, see: S. Sachdev, Nature Physics **4**, 173 (2008).
[3] A. W. Sandvik, Phys. Rev. Lett. **98**, 227202 (2007).
[4] P. Chandra and B. Doucot, Phys. Rev. B **38** 9335 (1988).
[5] E. Dagotto and A. Moreo, Phys. Rev. Lett. **63** 2148 (1989).
[6] H. J. Schulz, T. Ziman, and D. Poilblanc, J. Phys. I **6** 675 (1996).
[7] L. Capriotti, F. Becca, A. Parola, and S. Sorella, Phys. Rev. Lett. **87**, 097201 (2001).
[8] R. K. Kaul, R. G. Melko, and A. W. Sandvik, Annu. Rev. Cond. Matt. Phys. **4**, 179 (2013).
[9] R. G. Melko and R. K. Kaul, Phys. Rev. Lett. **100**, 017203 (2008).
[10] R. K. Kaul and R. G. Melko, Phys. Rev. B **78**, 014417 (2008).
[11] F.-J. Jiang, M. Nyfeler, S. Chandrasekharan, and U.-J. Wiese, J. Stat. Mech. (2008) P02009.
[12] J. Lou, A. W. Sandvik, and N. Kawashima, Phys. Rev. B. **80**, 180414(R) (2009).
[13] V. N. Kotov, D. X. Yao, A. H. Castro Neto, and D. K. Campbell, Phys. Rev. B **80**, 174403 (2009).
[14] A. W. Sandvik, Phys. Rev. Lett. **104**, 177201 (2010).
[15] A. W. Sandvik, V. N. Kotov, and O. P. Sushkov, Phys. Rev. Lett. **106**, 207203 (2011).
[16] A. Banerjee, K. Damle, and F. Alet, Phys. Rev. B **83**, 235111 (2011).
[17] Y. Nishiyama, Phys. Rev. B **85**, 014403 (2012).
[18] K. Damle, F. Alet, and S. Pujari, arXiv:1302.1408.
[19] T. Senthil, L. Balents, S. Sachdev, A. Vishmanath and M. P. A. Fisher, Science **303** 1490 (2004).
[20] T. Senthil, L. Balents, S. Sachdev, A. Vishwanath, and M.

P. A. Fisher, Phys. Rev. B **70**, 144407 (2004).
[21] A. B. Kuklov, M. Matsumoto, N. V. Prokof'ev, B. V. Svistunov, and M. Troyer, Phys. Rev. Lett. **101**, 050405 (2008).
[22] K. Chen, Y. Huang, Y. Deng, A. B. Kuklov, N. V. Prokof'ev, and B. V. Svistunov, arXiv:1301.3136.
[23] R. K. Kaul, Phys. Rev. B **85**, 180411(R) (2012).
[24] D. Friedan, Z. Qiu, and S. Shenker, Phys. Rev. Lett. **52**, 1575 (1984).
[25] J. Cardy, *Scaling and Renormalization in Statistical Physics* (Cambridge University Press, Cambridge, U.K., 1996).
[26] J. V. José, L. P. Kadanoff, S. Kirkpatrick, and D. R. Nelson, Phys. Rev. B **16**, 1217 (1977).
[27] P. Calabrese and A. Celi, Phys. Rev. B **66**, 184410 (2002)
[28] J. Ashkin and E. Teller, Phys. Rev. **64**, 178 (1943); C. Fan and F. Y. Wu, Phys. Rev. B **2**, 723 (1970).
[29] S. Wiseman and E. Domany, Phys. Rev. E **48**, 4080 (1993).
[30] S. Jin, A. Sen and A. W. Sandvik, Phys. Rev. Lett. **108**, 045702 (2012)
[31] A. Kalz and A. Honecker, Phys. Rev. B **86**, 134410 (2012).
[32] V. L. Berezinskii, Sov. Phys. JETP **32**, 493 (1970).
[33] J. M. Kosterlitz and D. J. Thouless, J. Phys. C **6**, 1181 (1973).
[34] M. Tsukamoto, K. Harada and N. Kawashima, J. Phys. Conf. Ser. **150**, 042218 (2009).
[35] A. W. Sandvik, Phys. Rev. B **59**, R14157 (1999).
[36] H. G. Evertz, Adv. Phys. **52**, 1 (2003).
[37] A. W. Sandvik, AIP Conf. Proc. **1297**, 135 (2010); arXiv:1101.3281.
[38] A. W. Sandvik, R. R. P. Singh, and D. K. Campbell, Phys. Rev. B **56**, 14510 (1997).
[39] M. E. Fisher and M. N. Barber, Phys. Rev. Lett. **28**, 1516 (1972).
[40] J. Lou, A. W. Sandvik, and L. Balents, Phys. Rev. Lett. **99**, 207203 (2007).
[41] K. Vollmayr, J. D. Reger, M. Scheucher, and K. Binder, Z. Phys. B **91**, 113 (1991).